# Operational Techniques in Microgravity for Cryogenic Fluid Management

Bryan D. Hoffman<sup>1</sup> and Jacob M. Brodnick<sup>2</sup>

NASA Marshall Space Flight Center, Huntsville, Alabama, USA

Management of cryogens in microgravity is a critical challenge for exploration missions to the Moon and Mars. Operational strategies to aid in cryogenic fluid management (CFM) are proposed and demonstrated using computational fluid dynamics simulations. Application of axial settling thrust is an essential – but potentially expensive – tool for CFM. Demonstrations show that its utilization and timing are important during certain unsettling events, such as engine cutoff. At other times, substantial savings can be realized by reducing the average acceleration (through pulsing thrusters, for example). If the metric for reaching a settled condition is a particular number of slosh periods, then fewer settling resources are needed with a lower acceleration. Alternatively, if a target wave amplitude is the settling objective, then a lower average acceleration will also allow for a higher allowable amplitude for the same heat transfer. Savings can also be obtained by rolling the vehicle, which can mitigate lateral slosh. Advantages and disadvantages of anti-slosh baffles are also discussed along with practical examples of their impact on CFM and ullage collapse. Ullage collapse examples are presented along with recommendations for slewing a vehicle with angular and translational acceleration to mitigate mixing between liquid and ullage.

## I. Nomenclature

 $\omega_n$  = angular frequency (natural)

R = tank radius a = acceleration T = time

 $Re_s$  = sloshing Reynolds number

b = wave amplitude  $\omega$  = angular frequency v = kinematic viscosity  $\gamma$  = slosh damping

d = baffle depth below the equilibrium liquid-vapor interface

## II. Introduction

Cryogenic Fluid Management (CFM) is an advancing field of study for liquid propellants enabling long term storage, control of thermodynamic conditions, and delivery to propulsion systems or tanks in all environments. CFM is essential for a sustainable presence on the Moon and crewed missions to Mars. Cryogens are favorable in aerospace applications due to their high specific impulse, noncorrosive qualities, and non-toxic exhaust gases, but are also vulnerable to evaporation or boiling over time, especially when mixed with warmer ullage gas through sloshing or inspace unsettling. CFM technologies, such as a cryocooler, thermodynamic vent system, or propellant management device, are specialized solutions for addressing the challenges posed by cryogenic propulsion. These technologies are critical in many contexts but leveraging body dynamics through the design of mission operations may be sufficient for some applications while avoiding the addition of some CFM dedicated technologies.

<sup>&</sup>lt;sup>1</sup> Computational Fluid Dynamics Engineer, Qualis Corporation/Jacobs Space Exploration Group

<sup>&</sup>lt;sup>2</sup> AST, Aerospace Propulsion Systems, NASA MSFC-ER42

In microgravity, liquid propellants tend to easily distribute throughout a tank, or unsettle, in response to applied forces. This behavior can be problematic for propulsion systems or propellant transfer between tanks due to the risk of vapor ingestion in feed lines or liquid ingestion in vent lines. Unsettling can also submerge ullage gas diffusers, hindering performance of pressurization systems not designed for that mode of operation. Moreover, unsettling and slosh can lead to unintentional mixing between a cryogenic liquid and a relatively warm ullage. This mixing generates heat and mass transfer between the two phases and can lead to ullage collapse, or the decline of ullage pressure towards saturated conditions. Unsettling events occur when there is a significant change in body force on the vehicle. Examples include engine cutoff or during attitude adjustments such as slews, maneuvers, and docking. Techniques for mitigating unsettling can be employed in the vehicle control system and used to levy constraints on the Concept of Operations (ConOps). Inefficiencies resulting in unsettling, slosh, or unintentional ullage collapse will need to be compensated by more resources or higher design margins for cryogenic systems. In-space propellant dynamics were investigated in the present work to demonstrate and address some of the design concerns discussed above with computational fluid dynamics (CFD) analysis.

# III. CFD Methodology

A cryogenic propellant tank representative of a large-scale main tank for an orbital rocket was selected for these analyses. The radius of the tank is 2 meters, the total height from end to end is 8 meters, the barrel section is 4 meters, and the forward and aft dome sections are 2 meter radius hemispheres. An illustration of the tank, along with coordinate axes and a 20% liquid fill level by volume, is shown in Fig. 1. The origin of the coordinate system is at the center of the tank, but the coordinate axes are labeled outside of the tank for visibility. A 20% liquid fill level was chosen to simulate the orbital environment following ascent, where most of the propellant has already been consumed and in-space maneuvers, thermal management, and docking with other spacecraft or stations are being evaluated.

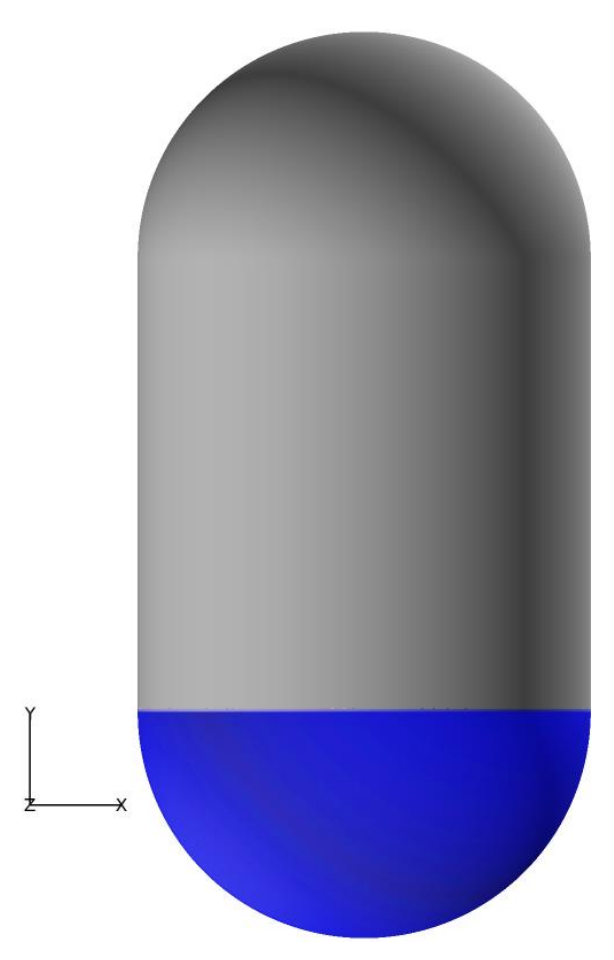


Fig. 1 Cryogenic propellant tank geometry and liquid fill level (blue).

Loci/STREAM, a pressure-based solver, was used in the preparation of these results. Typical simulation convergence within a timestep was achieved with reductions in residuals of at least three orders of magnitude for momentum and energy and four orders of magnitude for pressure. This level of convergence has been shown to yield negligible numerical error for other propellant tank applications [1] using the Loci/STREAM-Volume of Fluid (VoF) tool. The maximum time step was generally set to a value low enough to capture transient behaviors and further limited by the maximum Courant number (Co) in the computational domain. A maximum Co of 0.2 was used to determine the time step limit for the VoF solver.

For the problems addressed in this study, a laminar flow regime was sufficient to capture the bulk movement of propellant in the tank and a first-order upwind advection scheme was used for robust convergence across many cases. Flow was assumed to be compressible with heat transfer and phase change enabled for all simulations. Tank boundaries and baffles were modeled as adiabatic walls, so no heat transfer into or out of the tank was simulated. An implicit Hertz-Knudsen model for phase mass transfer within Loci/STREAM-VoF allows for evaporation and condensation at the liquid-vapor interface. The model determines the mass transfer rate using an accommodation coefficient that does not have a general empirical value. A value of 1e-3 was assumed for these analyses based on previous experience simulating tank self-pressurization and ullage collapse. This value is expected to err on the side of overestimating ullage collapse rates (i.e., over-predicting the decline of pressure). Ullage collapse trends are expected to hold so long as consistent accommodation coefficients are used for a set of simulations. CFD validation to empirical tests involving ullage collapse is currently in progress and should inform the proper coefficient for liquid oxygen (LOX) in this type of application.

## A. Computational Domain and Mesh

Multiple views of the mesh are presented in Fig. 2. The mesh is constructed of approximately 4 million hexahedral cells, which provide the highest quality results using the VoF module. A semi- block structured meshing approach was used to build the tank interior with a nearly uniform volume cell size throughout. Surfaces with unstructured quadrilateral cells were extruded vertically along the tank centerline and circumferentially around the tank exterior forming the tank volume.

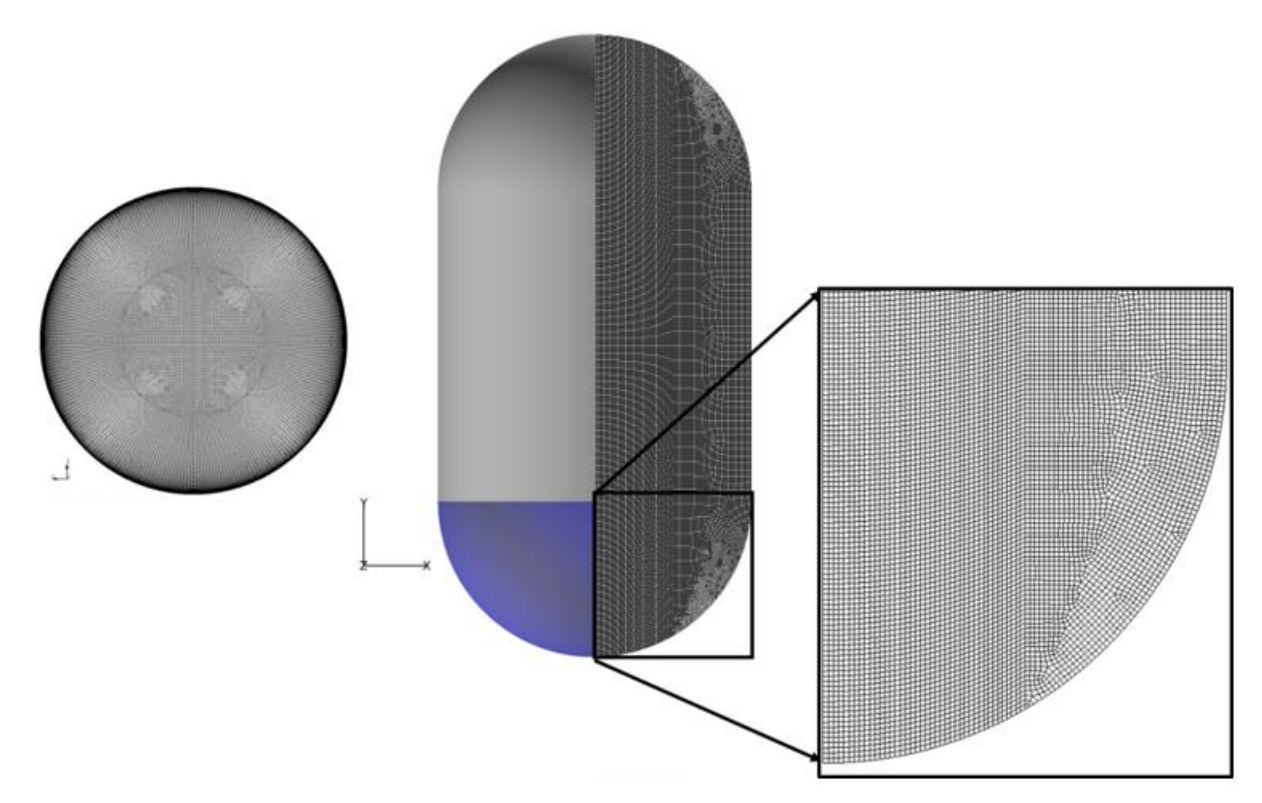


Fig. 2 Top view (looking down) and front view of the propellant tank mesh without a baffle.

Although many simulations used a bare tank without any internal structure, a baffle was included in others to highlight its effect on damping, unsettling, and ullage collapse. The baffle in Fig. 3 was positioned below the liquid-

vapor interface by 5% of the tank radius. This region provides high damping according to Miles' Equation [3], which has been replicated with CFD [2]. This height was chosen primarily to introduce damping into the system, not necessarily to maximize it. Since the baffle was in the aft dome, it was not purely horizontal, but angled to be orthogonal to the tank wall (which controls the liquid velocity vector). The width of the baffle (normal to the wall) is 10% of the tank radius. Finally, the thickness was set to a value of 1 inch for meshing simplicity. Three cells were placed across the thickness of the baffle. In practice, baffles are far thinner, but time steps significantly reduce for VoF methods when resolving small scale geometric features. The aim of this report is to reveal trends in bulk fluid dynamics rather than provide high fidelity solutions for a particular tank configuration. Coarse spatial resolution of an anti-slosh baffle is sufficient for capturing the settling, unsettling, and ullage collapse trends of interest.

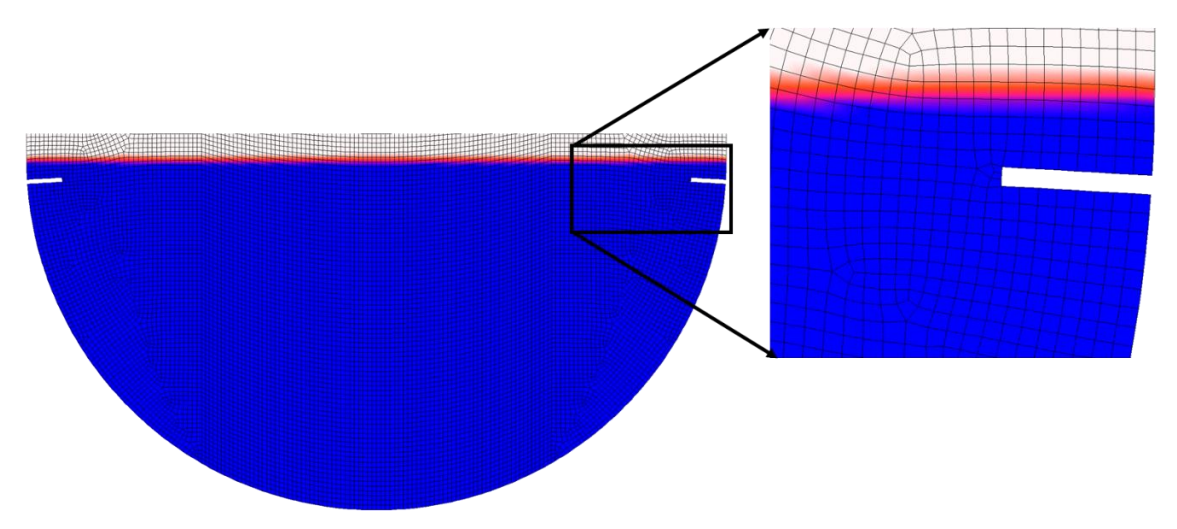


Fig. 3 VoF (liquid = blue, vapor = white) and mesh in the aft end of the tank with the anti-slosh baffle.

## **B.** Simulation Inputs

Liquid oxygen and gaseous oxygen (GOX) were selected as the fluids due to their commonplace usage in modern rocketry. The use of a single fluid for the ullage (vapor phase) simplifies the simulation methodology and provides an example of a spacecraft using autogenous pressurization rather than an ullage pressurized with an alternative fluid such as helium. Table 1 documents the fluid properties used for LOX and GOX in the settling studies as well as for engine cutoff and slews. All settling studies were performed with liquid and vapor saturated at 1 bar. Engine cutoff and slew, however, used an elevated tank pressure of 4 bar and an ullage temperature of 250 K. To provide a realistic transition between ullage temperature and liquid temperature, the liquid-vapor interface was set to a value of 105.73 K, which corresponds to the saturation temperature at 4 bar. The bulk liquid and ullage temperatures were then imposed 1 meter above and below the interface, with a linear interpolation of temperature in between.

Tuble 1 Third property inputs for Bork and Gork				
Fluid Property	Settling Studies		Engine Cutoff and Slew	
	LOX	GOX	LOX	GOX
Temperature (K)	90.0621	90.0621	90	250
Static Pressure (bar)	1		4	
Density (kg/m <sup>3</sup> )	1141.796	4.413	1142.772	6.192
Dynamic Viscosity (Pa*s)	1.953e-4	6.94e-6	1.962e-4	1.786e-5
Surface Tension (N/m)	0.013177	N/A	0.00937	N/A
Thermal Conductivity (W/m*K)	0.151028	0.008131	0.15135	0.02263
Bulk Modulus (N/m²)	512140982	N/A	515448746	N/A
Latent Heat (J/kg)	213239	N/A	191381	N/A
Cp (J/g*K)	1699	N/A	1697.3	N/A
Cv (J/g*K)	929.34	N/A	930.19	N/A

Table 1 Fluid property inputs for LOX and GOX.

The body rates, accelerations, and rotation center inputs for the engine cutoff and slew simulations were applied to the non-inertial reference frame holding the computational domain. The center point for the rotation rates was at an x, y, and z position of (0, 7, 0) meters, respectively. This represents a vehicle center of gravity (CG) in the upper dome of the tank, a common location for a large rocket which has a fuel tank forward of the oxidizer tank. The rotation rates and accelerations for the engine cutoff simulation are shown in Fig. 4. The cutoff starts at 4 seconds and the axial acceleration begins to drop from nearly  $30 \text{ m/s}^2$  to  $0 \text{ m/s}^2$  by 5.5 seconds. The angular rotation has an oscillatory pattern characteristic of flight data leading up to engine cutoff. In the lowermost plot, the y-axis is scaled down to show the magnitude and settling acceleration, if any.

Two slew profiles were created to compare the effects of translational acceleration on ullage collapse experienced during vehicle pitching. Both profiles involved moving the vehicle through a 100 deg rotation in 200 s. The same angular acceleration, performed over 20 s, was used to initiate and terminate the slew. In one case, there was no net translational acceleration applied to the vehicle, which may occur if a pair of forward and aft thrusters relative to the vehicle CG are fired with equal force in opposite directions. Alternatively, Fig. 5 depicts a case where there is a net translational acceleration in addition to angular acceleration. If thrusters are only used on one side of the vehicle at a time, this type of profile can be generated.

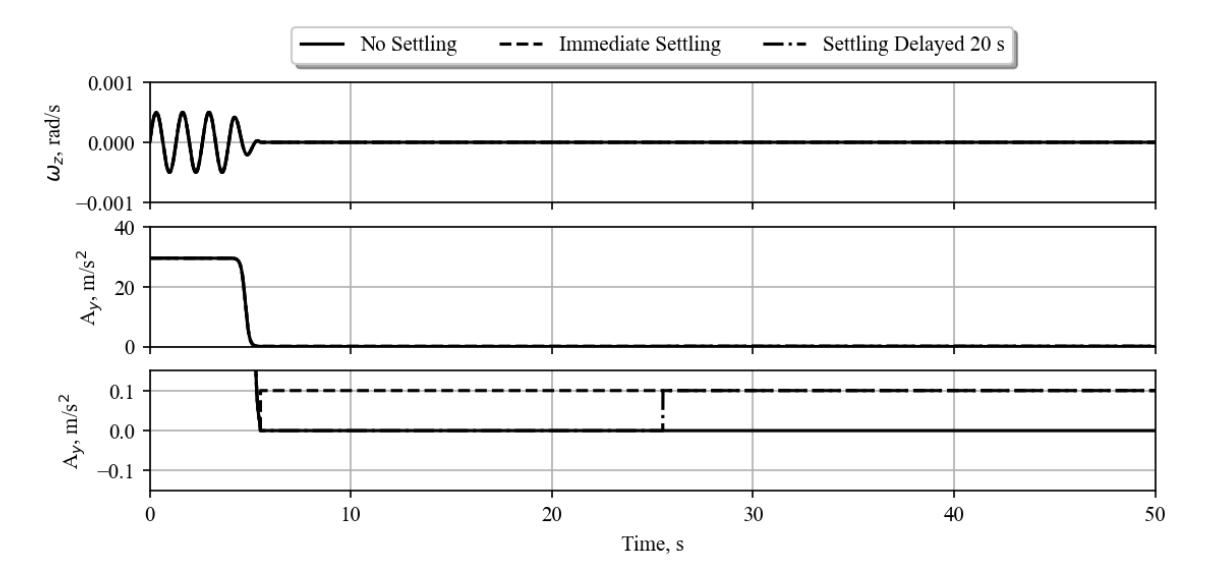


Fig. 4 Angular acceleration about the z-axis and axial acceleration (y-direction) for the engine cutoff studies.

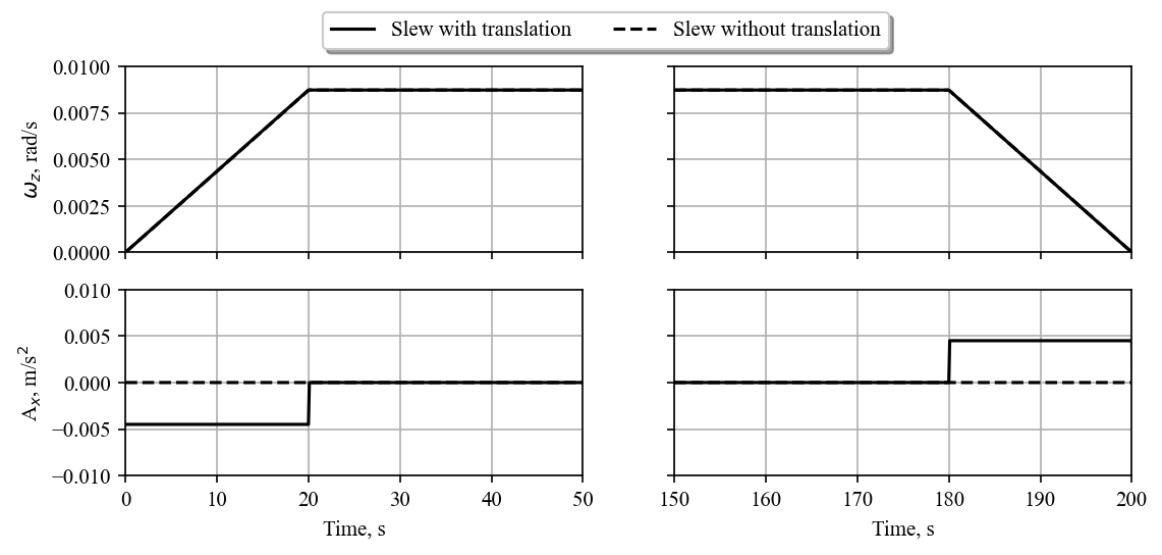


Fig. 5 Angular acceleration about the z-axis and axial acceleration (y-direction) for the slew variations.

### IV. Analysis

### A. Settling Thrust Optimization

To improve operations for CFM, a design tool was developed using CFD to inform tradeoffs between average acceleration, time spent firing thrusters, and total mission time. Pulsing, or introducing a time delay between thruster firings, is a common method for changing the average acceleration over a specified timeframe for fixed-output thrusters. Simulations show that, to achieve a quiescent state from an initially unsettled condition, pulsing increases the total ConOps time, but reduces the amount of time that thrusters must fire to reach the same fluid state. By reducing the amount of time spent accelerating, the efficiency of the operation increases, and mass dedicated to operating thrusters can be reduced. Alternatively, raising the average acceleration reduces operation time at the expense of thruster resources.

The underlying relationship can be explained using insight from mechanical model equations. The use of equivalent mechanical models, such as a spring-mass-damper or a simple pendulum model, for describing liquid slosh in a linear regime is well known. These models are typically used as inputs to Guidance, Navigation, and Controls (GN&C) analyses to characterize the slosh forces and moments imposed on a vehicle during flight. Traditional slosh models are not applicable in very low gravity or immediately after settling begins from a highly unsettled propellant state. However, slosh models can well represent propellant dynamics during settling and provide useful information about settling maneuver optimization. For a given tank geometry, an applied vehicle acceleration will result in a particular slosh frequency. The natural angular frequency ( $\omega_n$ ) scales with tank radius (R) and vehicle acceleration (R) according to the dimensionless parameter provided in Eq. (1). For a change in the vehicle acceleration, the natural angular frequency will respond according to the inverse of the square root. Assuming there is no change in tank radius, the natural angular frequency can be converted to wave period (R) by  $2\pi/\omega_n$  and simplified in Eqn. (2) to create an expression for the impact on total time to reach a given fluid state.

$$\omega_{n,1}^2 \frac{R_1}{a_1} = \omega_{n,2}^2 \frac{R_2}{a_2} \tag{1}$$

$$\frac{T_2}{T_1} = \sqrt{\frac{a_1}{a_2}} \tag{2}$$

The efficiency gain observed when lowering the average acceleration is a consequence of Eqn. (2). If  $T_1$  is the total time required to settle at acceleration  $a_1$ , then reducing the average acceleration  $(a_2)$  to half of  $a_1$  would only increase the total time,  $T_2$ , by the square root of two. However, since the thruster duty cycle (i.e., the time actively firing thrusters relative to the total time) is still directly proportional to the ratio of the accelerations, a net gain results; the mass used to settle the liquid is reduced by a factor of  $\sqrt{2}/2$ , or 29.3%. This provides a favorable optimization mechanism for mission planners during the design of the ConOps. If similar damping occurs over the same number of wave periods, operations can be structured to use less resources.

To confirm this behavior, CFD data capturing the total time was simulated for five different average accelerations, or duty cycles. For simplicity, the 100% duty cycle was chosen to be the 0.10 m/s² acceleration, and all other average accelerations are expressed as a percentage of this value. In Fig. 6, the lateral (x-direction) displacement of the liquid CG is plotted. Each marker represents a peak in the wave amplitude, or half a slosh period, as liquid oscillates from one side to the other. The cryogen was initially placed completely offset on one side of the tank, similar to what may be experienced following a pitch or yaw maneuver. Applying an axial acceleration with liquid offset to one side immediately starts a lateral slosh motion. The first two wave periods are defined by nonlinear sloshing characteristics. The high wave amplitudes result in significant splashing and higher order mode shapes, increasing damping. After approximately three wave periods, the wave amplitude has decreased to a degree that very little damping takes place in the bare tank (without baffles) pictured in Fig. 2.

Notably, the trend with each acceleration magnitude is very similar. The markers at each half period are at approximately the same  $X_{CG}$  values, with only slight differences from one case to another. All cases enter a steady sloshing condition with CG displacements of about 0.2-0.25 m. As expected, the time it takes to complete these oscillations is the primary distinction. This provides verification that the time to achieve a particular slosh amplitude, or to reach a steady condition, can be approximated as a function of number of slosh periods.

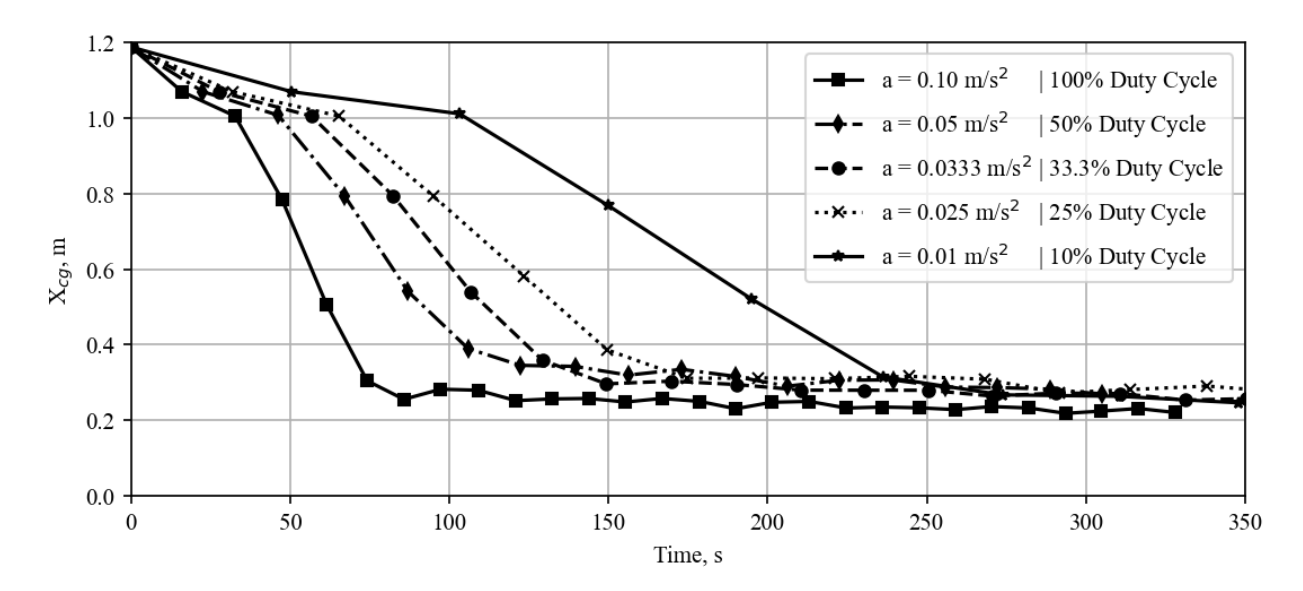


Fig. 6 Transient comparisons of acceleration magnitude on lateral liquid CG displacement.

With settling time given as a function of period, or frequency, the relationship in Eq. (2) can be leveraged to create the settling design tool in Fig. 7. A prediction for the total settling operation time (dashed line) is co-plotted with the time spent actively firing thrusters (dotted line), which is simply the total mission time multiplied by the fractional duty cycle. As noted in the CFD results from Fig. 6, very little damping occurs beyond about three wave periods, so this was specified as the metric for achieving a settled state. The times to reach this metric for each acceleration magnitude are also overlaid as square markers. The time spent accelerating corresponding to each CFD value is given by an x. For example, at the 100% duty cycle acceleration, the time to reach three wave periods and the time spent actively firing is about 80 s, according to Fig. 6, so that is the time annotated and denoted by the square marker there.

The consistency between the predictions (lines) and CFD results (markers) verifies Eqn. (2). On the second y-axis, the performance relative to the 100% duty cycle acceleration is shown and these values are annotated beside the time in seconds at each CFD point. As forecasted previously, a reduction in the average acceleration by half will produce a settling mass reduction of 29.3%. The CFD result reports a savings within 1% of this prediction. This tool can be used by mission planners to evaluate the total time needed for liquid aggregation and minimize the propellant expended to perform the aggregation.

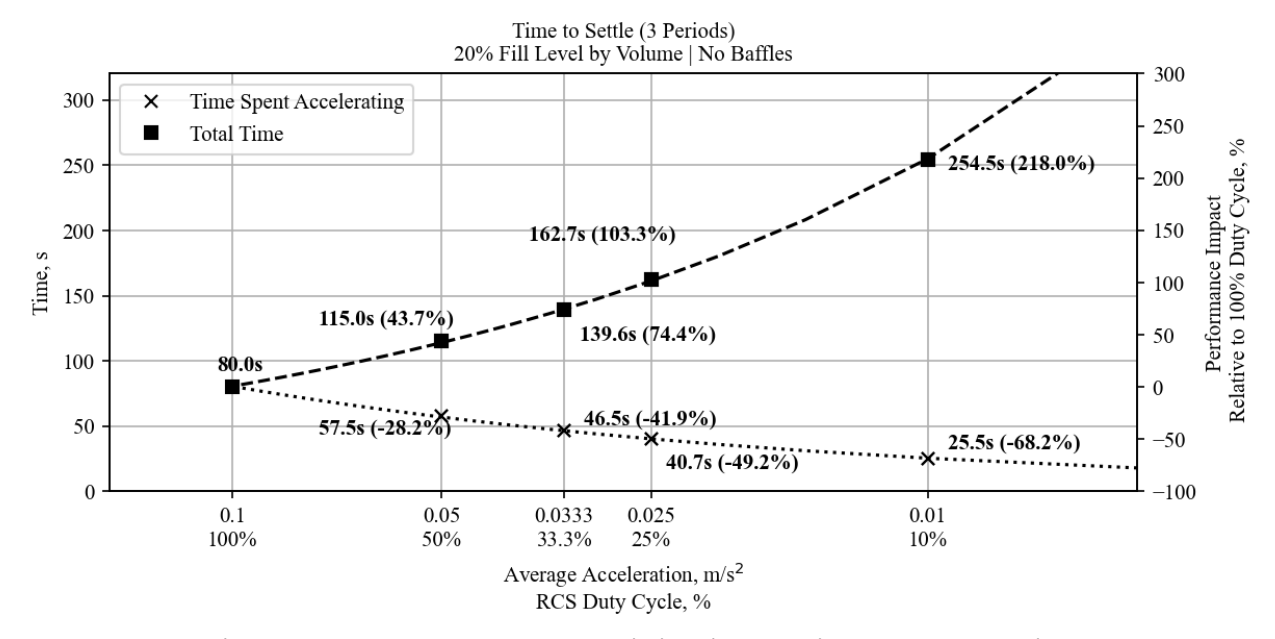


Fig. 7 Thruster duty cycle vs. total mission time and time spent accelerating.

While simple and convenient, here are several limitations to this methodology. One is the applicable range of the performance benefit. If the duty cycle is too low – such that the time between pulses is on the order of the slosh period – the average acceleration is no longer an effective approximation. Furthermore, if the Bond number, which is the ratio between the thrust and surface tension, is below about 10, then the liquid will tend to creep up along tank walls rather than maintain its settled condition [4]. This higher influence of surface tension at low accelerations can be exacerbated if there is a lot of internal structure in a tank, especially propellant management devices. It should also be reemphasized that the design tool in Fig. 7 is dependent upon at least on calibration point. Either test data or an analysis result may be used to provide a data point from which Eq. (2) can be extrapolated. A calibration point will be needed for each tank configuration and initial fluid state that is to be considered.

An additional benefit to reducing settling acceleration is the potential reduction of heat transfer for the same sloshing wave amplitude. Ludwig, Dreyer, and Hopfinger state that the heat transfer is a function of the wave amplitude, captured by the correlation between the sloshing Nusselt number and the sloshing Reynolds number ( $Re_s$ ) [5]. A target sloshing Reynolds number may be chosen by engineers to obtain an acceptable level of heat transfer. The authors introduce the expression in Eqn. (3) for sloshing Reynolds number as a function of wave amplitude (b), angular wave frequency ( $\omega$ ), and kinematic viscosity (v). When lowering the applied acceleration, the angular wave frequency will decrease according to the relationship in Eqn. (1). Therefore, with a target value of the sloshing Reynolds number, the wave amplitude will be greater for a lower acceleration. For CFM engineers using slosh amplitude as a metric for achieving a settled state, these important relationships indicate that less stringent amplitudes are needed if settling is performed at lower average accelerations (i.e., at lower duty cycles of reaction control system (RCS) thrusters).

$$Re_s = b^2 \frac{\omega}{v} \tag{3}$$

For example, Ludwig, Dreyer, and Hopfinger produced a correlation of empirical results showing that effective diffusivity (sloshing Nusselt number) does not change due to sloshing until reaching a critical sloshing Reynolds number  $(Re_s)_c$  of  $4000 \pm 20\%$  [5]. Below this critical number, sloshing does not noticeably increase heat transfer and pressure change in a cryogenic tank. This is useful in a situation where a tank needs to be settled to improve efficiency, or lower the condensation rate, of a subsequent pressurization operation. Consequently, the critical sloshing Reynolds number may be a practical target for determining the amount of resources to expend on settling. Alternatively, it could be used in the design process to specify the hardware needed to generate the damping for a required settling budget. The plot in Fig. 8 illustrates the degree to which slosh wave amplitude changes with acceleration magnitude.

It should be noted that the referenced work [5] did not include acceleration magnitude sensitivity but rather wave amplitude, fluid, and tank size variation. Applicability of the subject work to acceleration magnitude variations is an active area of study.

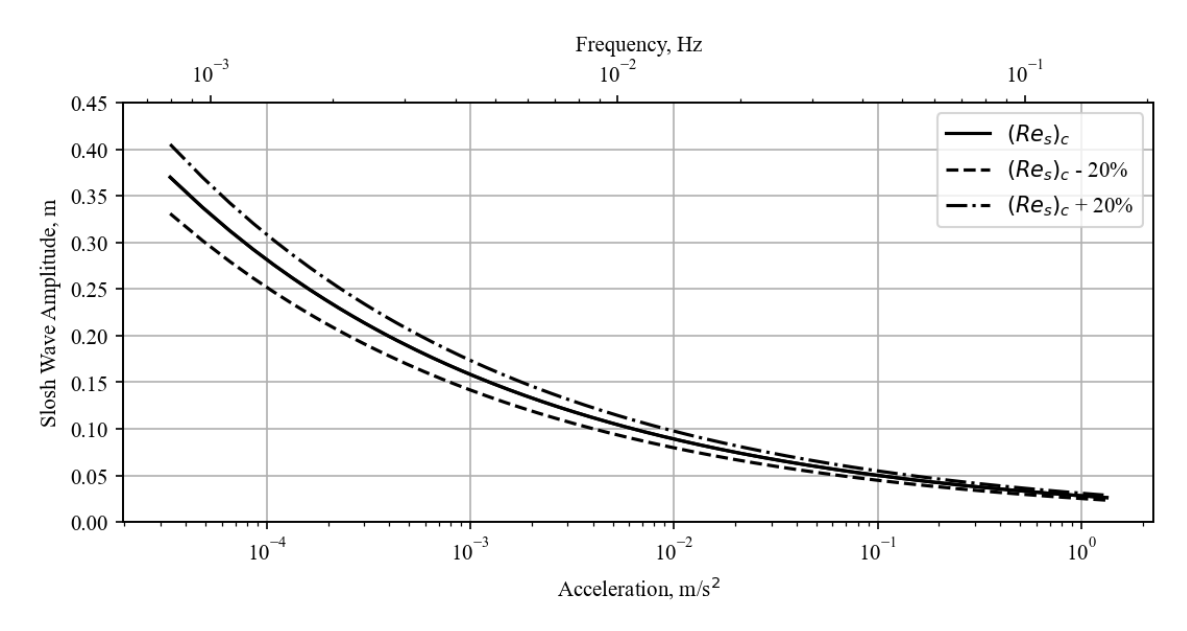


Fig. 8 Slosh Wave Amplitude vs. Angular Frequency and Acceleration at  $(Re_s)_c = 4000 \pm 20\%$ .

#### B. Lateral Slosh Reduction through Vehicle Roll

One technique to mitigate unsettling is to induce a roll to minimize lateral slosh, leading to improved settling efficiency prior to venting, delivery of propellant to engines, or transfer to another tank. In architectures without PMDs, an acceleration or thrust is generally required for liquid aggregation. The acceleration is commonly produced by RCS thrusters which are allotted a budget of propellant mass for the purpose of settling cryogens. Rolling a vehicle not only acts as a passive thermal control for reducing boil-off (e.g., the so-called "barbecue" roll as applied in the Apollo missions), but also thoroughly distributes the propellant against the tank boundaries at a low cost. Once the vehicle is spun up to its desired rotation rate, a body force is consistently available for no additional fuel spent. Once liquid is well-distributed, the liquid center of mass is positioned close to the tank axis. This positioning aids in partially cancelling lateral slosh forces that can increase the propellant mass and the time required to reliably settle the liquid.

Using CFD with a VoF approach, tank simulations were performed to show that propellant savings may be achieved by incorporating a roll before conducting settling operations. Axial and transverse CG displacements are plotted in Fig. 9. All cases were settled at the same acceleration magnitude of  $0.10 \text{ m/s}^2$  starting at t=0 s. The difference between the cases shown is the initial condition of the liquid. The "lateral offset" is the same case shown in Fig. 6, where the liquid is initially positioned entirely on one side of the tank and near the aft end. In this case, the initial lateral CG position ( $X_{CG}$ ) is 1.2 m. The "circumferentially distributed" case corresponds to a steady-state roll, where all the liquid creates a cylinder around the tank boundaries. The initial lateral CG position in this case is 0 m. The last case, "partially offset," includes liquid on all sides of the tank, but it is biased towards one side, reflected in the initial later CG position of 0.7 m.

The two plots illustrate the effect of liquid position on slosh. With liquid entirely on one side, there is very little to obstruct lateral motion except for the interaction with the walls. With a partially offset CG, liquid converges on the aft end from multiple sides and effectively provides additional damping. When liquid is completely distributed around the circumference, nearly all lateral forces are offset. Although the latter case appears to be considerably better than the others, the CG displacements do not reveal the significant axial slosh motion present during settling at high acceleration magnitudes. Thus, a balance should be struck between minimizing the lateral slosh (and therefore, the settling resources required) and the vertical slosh modes. This technique may be particularly beneficial when combined with a propellant management device and low settling acceleration, increasing the influence of surface tension and potentially deterring axial slosh.

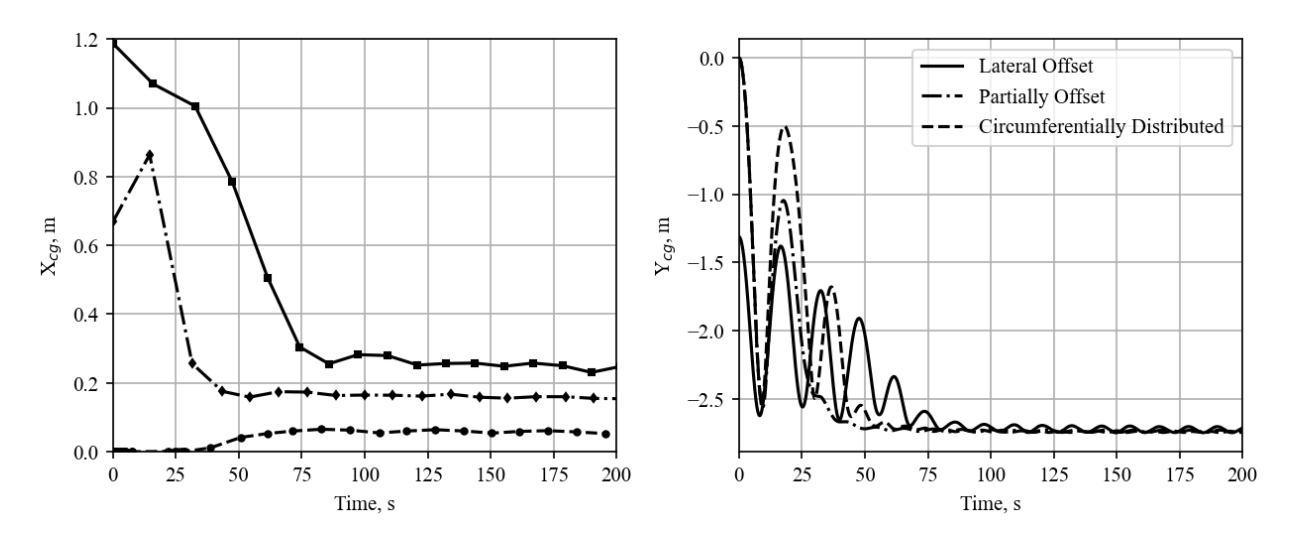


Fig. 9 Axial and lateral CG displacements for liquid during a steady-state roll, transient roll, and without roll.

## C. CFM Impact of Anti-Slosh Baffles

Anti-slosh baffles are commonly used to introduce damping into cryogenic propellant tanks. In the absence of a baffle or other internal structures, persistent slosh is expected. Fig. 6 illustrates the problem encountered by bare wall tanks. When slosh waves are large, the chaotic and nonlinear behavior provides a degree of natural damping that reduces lateral displacements rapidly. Upon reaching lower amplitudes, shear stresses within the liquid and along the wall are small yielding little damping of slosh waves. Persistent sloshing may cause inefficiencies or failures in

propellant delivery and pressurization. Additionally, halting settling during slosh motion will inevitably lead to propellant unsettling due to any residual liquid momentum effectively undoing the settling maneuver.

Anti-slosh baffles are used to dissipate slosh wave energy by providing a mechanism for vortex generation which yields higher damping at all wave amplitudes compared to a bare tank. In this way, a baffle or set of baffles can enable efficient settling to propellant states otherwise unobtainable for bare tanks over reasonable operation durations. Not only do they reduce slosh within the system, but they can also serve as a physical barrier, or deflector, to keep liquid from creeping along tank walls in microgravity.

The contrast of a baffled tank and an unbaffled tank is shown in Fig. 10. The unbaffled tank from Fig. 6 is plotted next to the baffled configuration described in the Computational Domain and Mesh section. Immediately upon settling, there is a significant reduction in the CG displacement. Some of this impact is dependent on the geometry configuration; baffles that deflect a wave across the tank and cause it to re-contact the liquid out of phase will result in higher apparent damping. However, the most noteworthy impact is the continued decrease in the amplitude over time. The damping  $(\gamma)$  is described by Eqn. (4), the Miles equation for a straight cylinder [3], as a function of depth below the equilibrium liquid surface (d), tank radius (R), slosh amplitude (b), and an area blockage term (a).

$$\gamma = 2.83e^{-4.6(\frac{d}{R})}a^{\frac{3}{2}}\sqrt{\frac{b}{R}}$$
 (4)

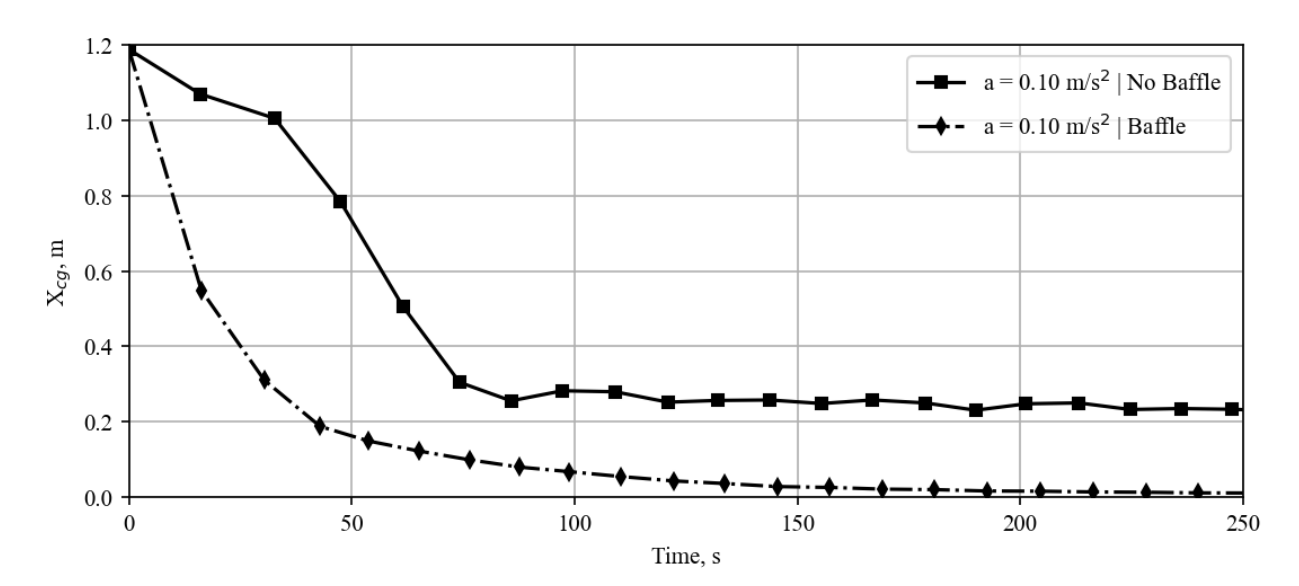


Fig. 10 Transient comparisons of baffled and unbaffled tanks on lateral liquid CG displacement.

The disadvantage to baffles, aside from the dry mass they add to a rocket, is that they may induce liquid breakup during maneuvers, docking, or after engine cutoff events. The additional breakup is harmful from a CFM perspective since it will accelerate ullage collapse through liquid mixing with warmer ullage vapor. To show this disadvantage, cross sectional contour plots showing the liquid position in the two simulations from Fig. 10 are compared in Fig. 11. With an unbaffled tank, the liquid momentum carries the propellant up the opposite wall once the axial acceleration of 0.1 m/s² is applied. However, the liquid stays largely contiguous as it moves. Conversely, the liquid striking a baffle has sufficient energy to overcome surface tension, leading to droplets or globules of liquid redirected away from the tank wall and into the ullage. Note that these simulations do not have sufficient mesh resolution to capture the smallest droplets formed by the slosh wave breaking which could lead to significantly more spray than is predicted. Liquid broken up in this way experiences more heat transfer due to enhanced exposed surface area with the hot gas.

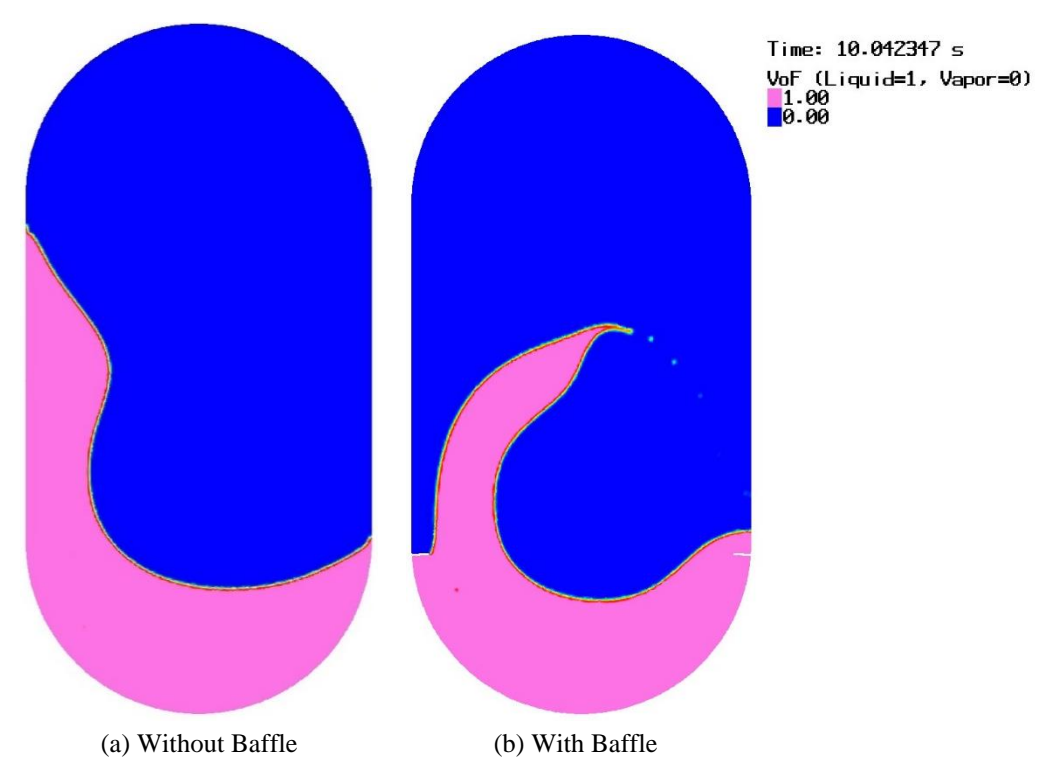


Fig. 11 Cross-section of VoF after 10 s for a tank with and without baffles (z = 0 plane).

#### D. Ullage Collapse Mitigation

Managing ullage conditions in a cryogenic propellant tank is a substantial challenge in a microgravity environment. Liquid position in microgravity is governed by surface tension – normally a very weak force – so even small accelerations can lead to significant motion that may be uninhibited for long durations. These accelerations may come from spacecraft attitude adjustments to align with other vehicles, to prepare for orbital changes, or to reduce heat transfer (e.g., maintaining a sun-pointing orientation). The most reliable way of actively controlling the propellant in these cases is to apply axial settling acceleration. However, this solution can be costly, and methods for minimizing these resources are documented in a prior section. Alternative methods for reducing mixing between the ullage and liquid during an attitude change can also serve to save settling resources.

Operating thrusters with equal force outputs on either side of the vehicle CG can be used to produce purely rotational motion. In this scenario, the vehicle rotates around its CG, but the CG remains stationary relative to the vehicle trajectory prior to the maneuver. The tank walls will move relative to the liquid. The relative motion is primarily a function of the angular acceleration and the centripetal acceleration, determined by the rotation rate. To minimize ullage collapse with this type of rotation, the angular acceleration and maximum rotation rate should be kept relatively low (long time frames). However, there is dependency on the location of the CG. If it is forward of the liquid, a faster rotation rate will produce a centrifugal force which acts as a settling mechanism. This will be reversed in the case where the CG is aft of the liquid and the liquid is initially settled in the aft end of a tank.

On the other hand, if unequal forces are used to generate a rotation about the CG, they will produce both an angular acceleration and a translational acceleration. The addition of translational acceleration can be leveraged to counteract the tendency for liquid to move up the sides and around the tank. The inputs for the two cases chosen to demonstrate this benefit are shown in Fig. 5. In the simulation without translation, a consistent drop in both mean pressure and ullage temperature was observed in Fig. 12. The decline accelerated around the 200 s mark when the mixing increased due to the termination of the slew. Condensation takes place for most of the maneuver, contributing to a reduction in the gas mass and the pressure.

However, liquid motion is arrested and significantly reduced when translational acceleration is included. In Fig. 13 and Fig. 14, liquid position over the first 200 s is shown. The angular acceleration tends to move the liquid in a clockwise rotation around the tank. If the translational acceleration opposes this tendency at a suitable magnitude though, the motion can be offset, such as in Fig. 13 at the 100 s mark. Centrifugal force from the vehicle rotation influences the position thereafter, aiding in containment of the liquid propellant. Balancing the angular acceleration

and translational acceleration provides the savings with this operational technique. Challenges in this technique arise when thruster combinations cannot easily balance the rotational forces. Furthermore, additional attitude corrections could be necessary to counteract the effects of translation on vehicle trajectory.

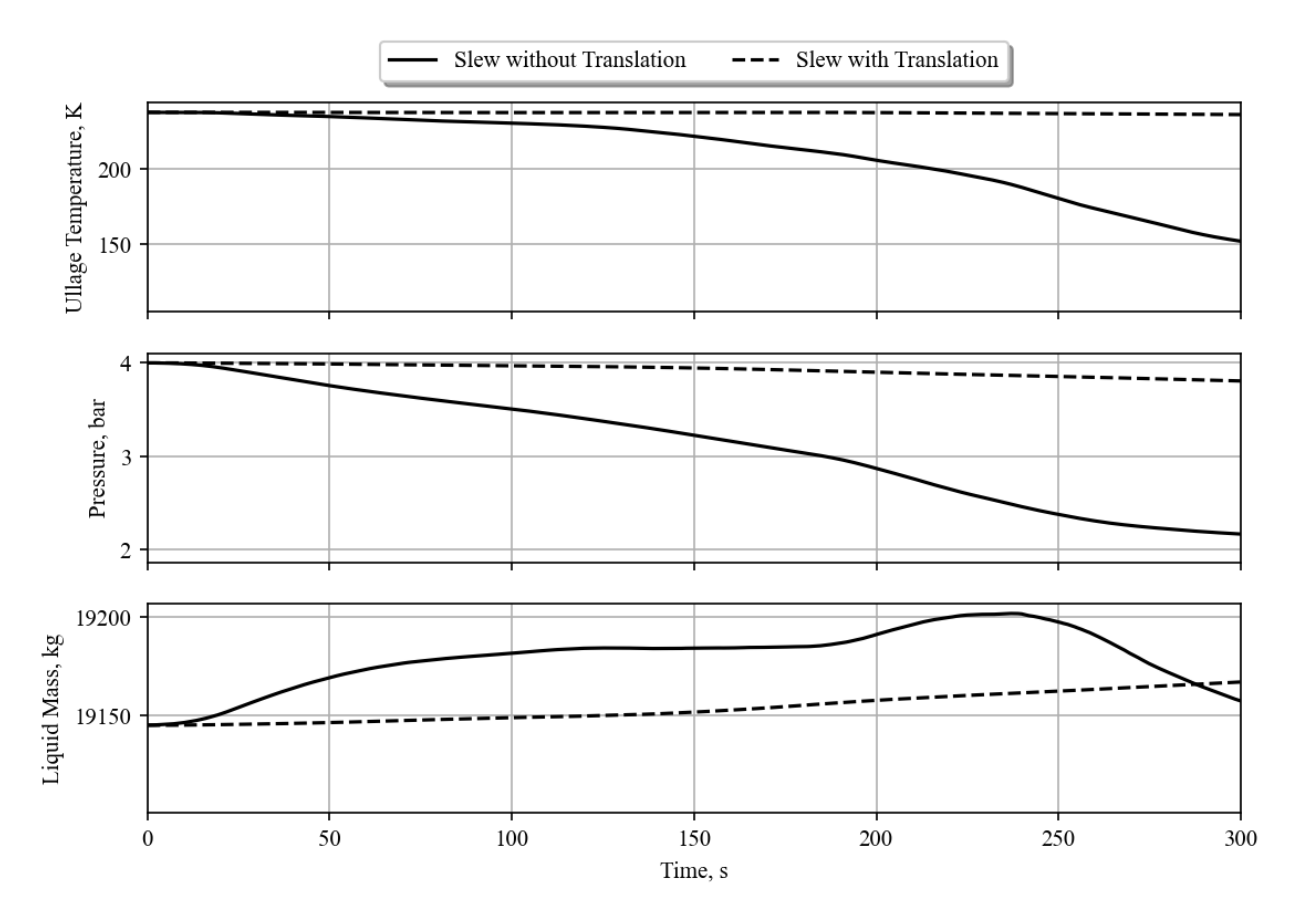


Fig. 12 Ullage temperature, tank pressure, and liquid mass for a slew with and without translation.

A similar study was performed for ullage collapse following engine cutoff. With an engine cutoff event, the precise motion of the vehicle is not known a priori. Vehicle accelerations may occur in all six degrees of freedom. While thrusters are used to correct for these accelerations and maintain trajectory, they are reactionary and not aimed at minimizing liquid unsettling. Consider the engine cutoff profile illustrated in Fig. 4. After several oscillations in the transient leading up to shutdown at 5.5 s, the rotation rate is steadily brought to zero at the time the axial acceleration is null. Nevertheless, the liquid carries momentum from sloshing which will collapse the ullage if no mitigation strategies are employed. To that end, axial acceleration remains the primary tool to combat ullage collapse.

Ullage temperature, pressure, and liquid mass for three engine cutoff variations are displayed in Fig. 15. All three of the cases include the baffle outlined in section III to capture the gradual decay of wave amplitude once the 0.1 m/s² axial acceleration begins. Without settling, the pressure and ullage temperature decline towards saturated conditions before beginning to asymptotically approach a value of around 2 bar. Liquid in this context is circumnavigating the tank, with warm ullage primarily in the center of the vessel. The tank is not yet fully mixed but is approaching a pseudo steady condition. The remaining two cases are intended to show the impact of when axial acceleration is applied. In the delayed case, the settling thrust is activated at the 25.5 s mark, 20 s after the engines are completely shut down. Around the 35 s mark presented in Fig. 16, this happens to be slightly worse for ullage temperature than the unsettled case, because liquid contacts the baffle and it is detached from the wall, cooling the hot gas in the center of the tank. Nevertheless, this deficiency is short-lived, and the aggregation of liquid at the bottom of the tank outperforms the case without settling in the long term. Immediately applying axial acceleration after cutoff clearly provides the most effective technique for preserving ullage conditions. Mean ullage temperature is relatively unaffected, indicating that the pressure loss communicated in Fig. 15 is due, in large part, to the condensation predicted by the mass transfer model.

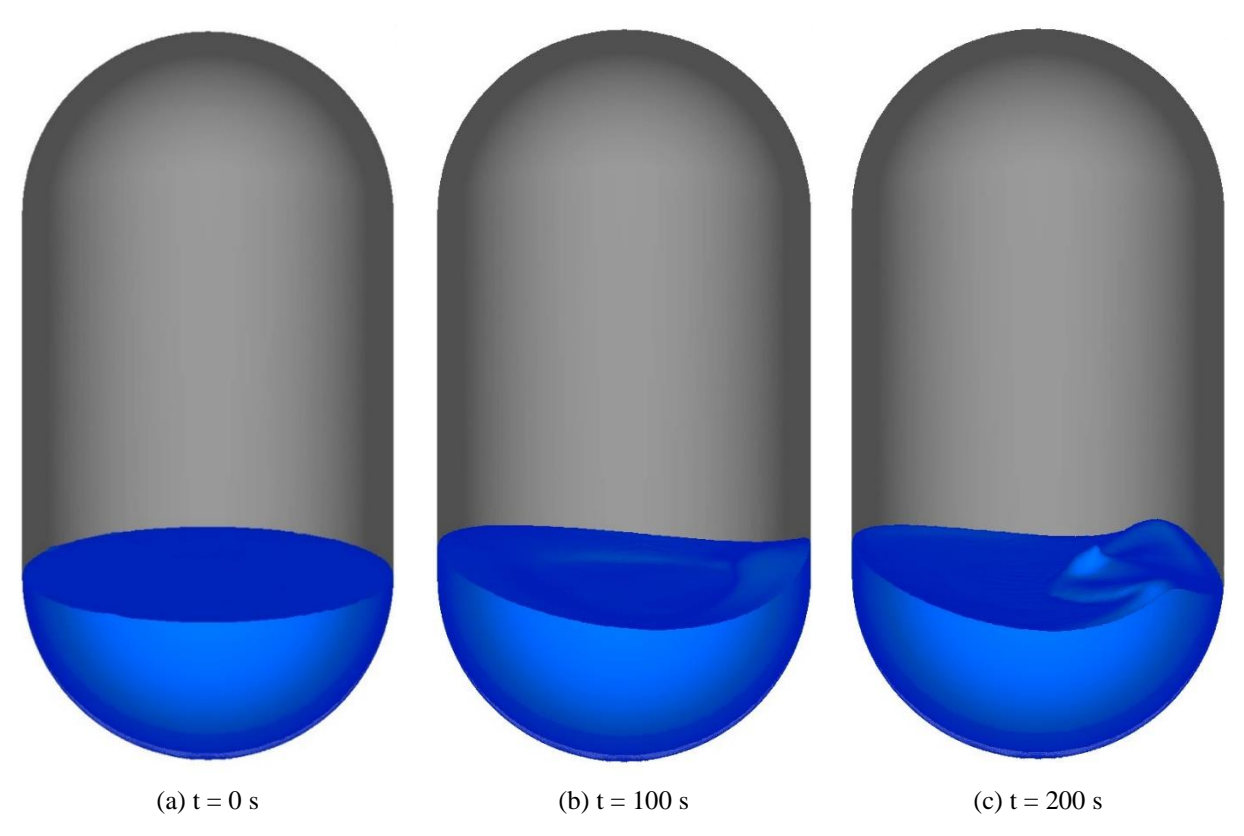


Fig. 13 Liquid positions at 0, 100, and 200 s after slew initiation with translation.

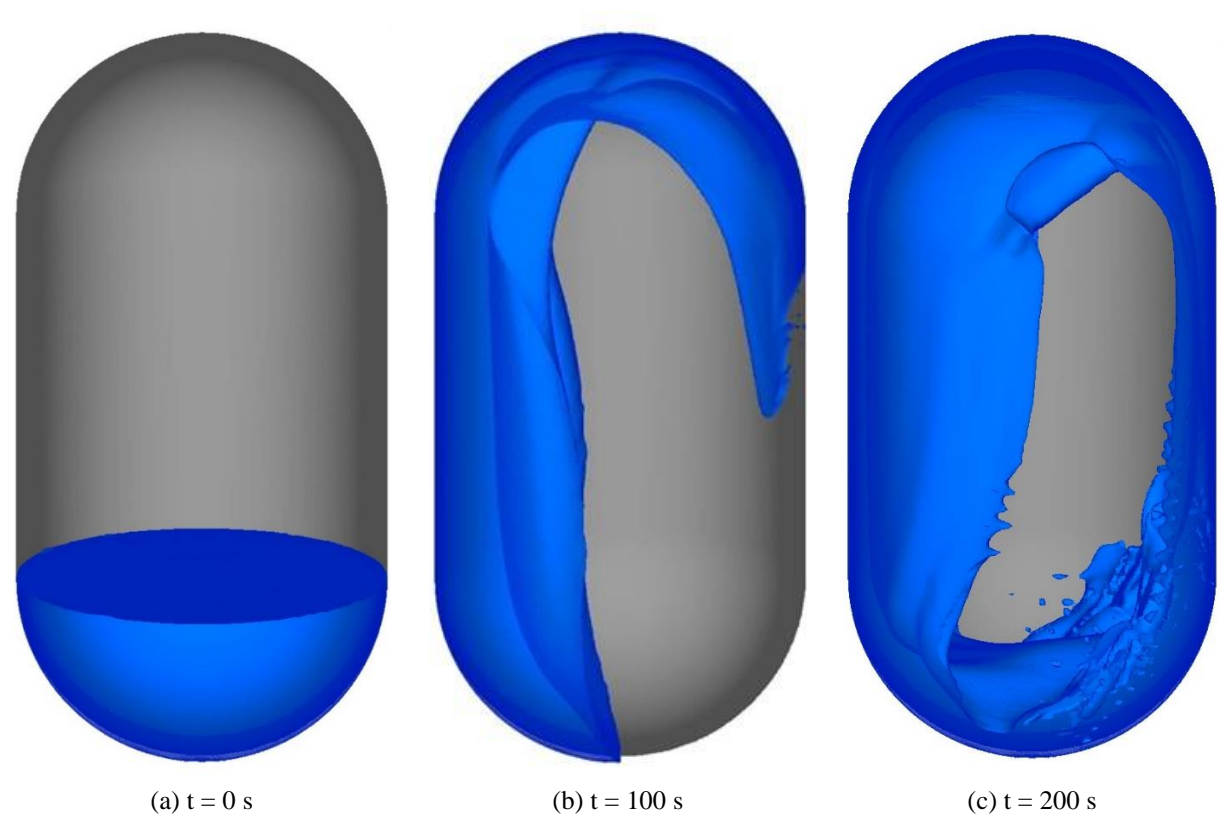


Fig. 14 Liquid positions at 0, 100, and 200 s after slew initiation without translation.

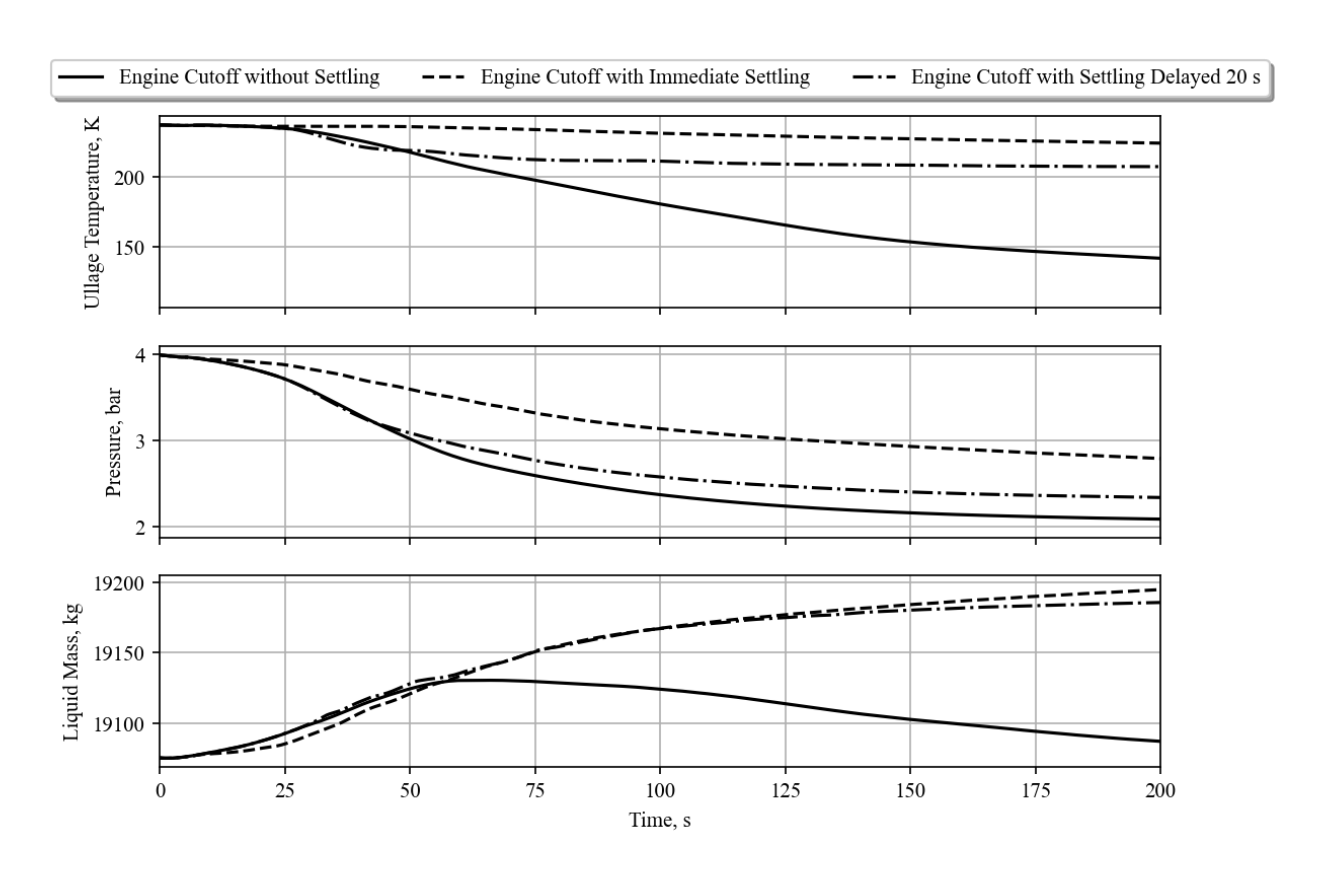


Fig. 15 Ullage temperature, tank pressure, and liquid mass for engine cutoff with settling variations.

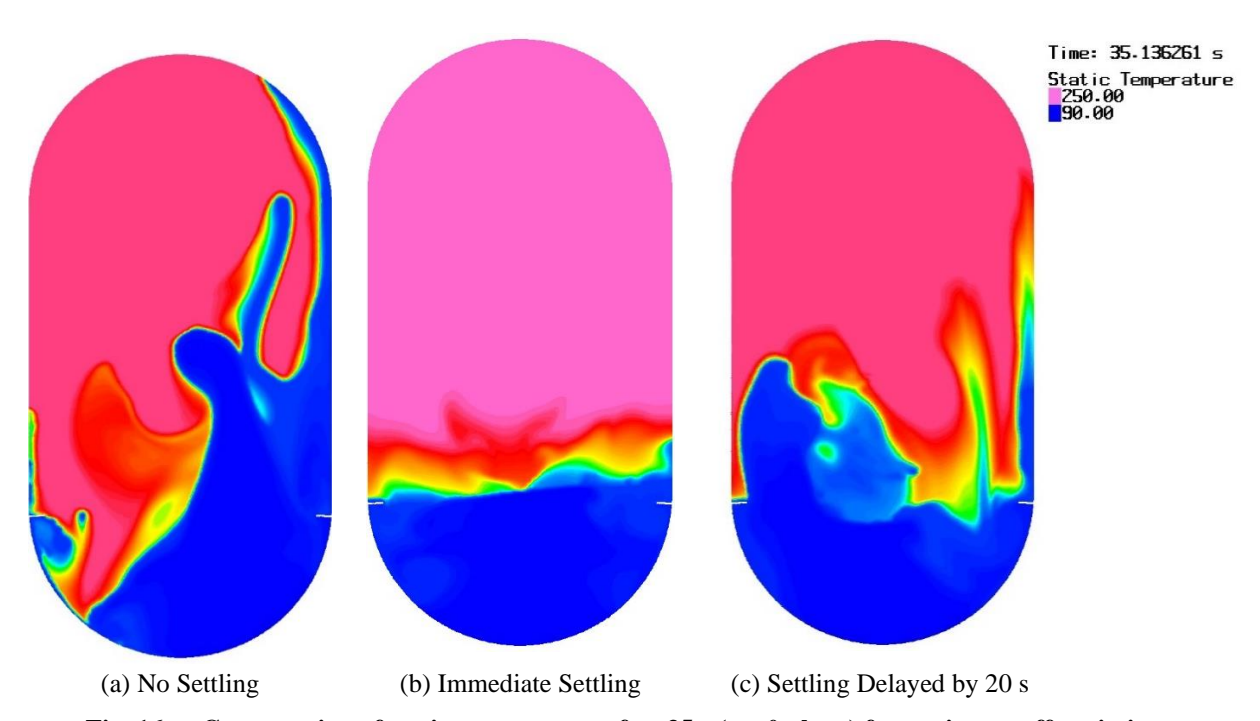


Fig. 16 Cross-section of static temperature after 35 s (z = 0 plane) for engine cutoff variations.

#### V. Conclusion

CFD simulations were utilized to demonstrate operational techniques for improving in-space management of cryogens within large propellant tanks. Strategies for addressing CFM concerns around settling optimization, engine cutoff events, and slew maneuvers were discussed as well as the influence of anti-slosh baffles. To minimize ullage collapse in a tank during a pitch or yaw, the design of the rotation may be planned in a manner which offsets as much of the disturbance to the liquid as possible. This can be achieved by controlled firing of one or more thrusters to introduce a translational acceleration which counteracts the effects of the required angular acceleration. In an engine cutoff scenario, where the forces and moments on a vehicle are not as defined, axial acceleration should be applied as soon as possible to avoid significant reductions in pressure and temperature. Baffles can assist in preserving ullage conditions by removing slosh from the system but can also expedite ullage collapse if axial acceleration is not introduced promptly.

Bulk propellant dynamics were found to be insensitive to settling acceleration magnitude. Leveraging this information enables extrapolation of a single test dataset or analysis result of propellant settling time to other acceleration magnitudes creating a settling maneuver design tool. The result demonstrates that while maneuver duration increases as settling acceleration decreases, the time spent settling, and thus the thruster working fluid mass, is reduced. This trend holds for a given tank configuration and initial condition. Varying the initial condition was also shown to affect settling time. In particular, rolling a vehicle to evenly distribute propellant circumferentially around the tank inhibited lateral slosh following settling instead yielding symmetric slosh motion. Striking a balance between lateral and circumferential initial propellant distribution was found to minimize settling time to reach a particular slosh wave amplitude.

## Acknowledgments

The authors would like to thank members of the Fluid Dynamics Branch (ER42) at the Marshall Space Flight Center, including Brandon Williams, Chintan Patel, Hong Yang, and Marco Sansone. In addition, the authors would like to thank the engineers at Space Exploration Technologies (SpaceX) and the Glenn Research Center for partnering in many tasks related to this product. Resources supporting this work were provided by the NASA High-End Computing (HEC) Program through the NASA Advanced Supercomputing (NAS) Division at Ames Research Center.

#### References

- [1] Brodnick, J.M., Westra, D.G., Eberhart, C.J., Yang, H.Q., and West, J.S., "Wave Amplitude Dependent Engineering Model of Propellant Slosh in Spherical Tanks," *JANNAF PIB/11th MSS/9th LPS/8th SPS Meeting*, December 2016.
- [2] Yang, H.Q., West, J., "Validity of Miles Equation in Predicting Propellant Slosh Damping in Baffled Tanks at Variable Slosh Amplitude," *AIAA SciTech Forum/2018 AIAA Aerospace Sciences Meeting*, January 2018.
- [3] J. W. Miles," Ring Damping of Free Surface Oscillations in a Circular Tank," *Journal of Applied Mechanics*, vol. 25, no. 2, June 1958, pp. 274-276.
- [4] Hochstein, J.I., and Chato, D.J., "Pulsed Thrust Propellant Reorientation: Concept and Modeling," *Journal of Propulsion and Power*, Vol. 8, No. 4, July-Aug., 1992.
- [5] Ludwig, C., Dreyer, M.E., and Hopfinger, E.J., "Pressure Variations in a Cryogenic Liquid Storage Tank Subjected to Periodic Excitations," *International Journal of Heat and Mass Transfer*, Vol. 66, 2013, pp. 223-234.